American Mineralogist, Volume 73, pages 224–231, 1988

Computer simulation of the structure, lattice dynamics, and thermodynamics of ilmenite-type $MgSiO_3$

ALISON WALL, GEOFFREY D. PRICE
Department of Geological Sciences, University College London, Gower Street, London WC1E 6BT, U.K.

ABSTRACT

The $(Mg,Fe)SiO_3$ phase of ilmenite structure type may be a constituent of the Earth's mantle, occurring at the base of the transition zone or the top of the lower mantle; therefore, a knowledge of its elastic and energetic properties is essential if we are to understand phenomena such as mantle rheology and the cause of seismic discontinuities. However, considerable experimental problems are involved in the study of this phase, and, hence, atomistic computer-simulation techniques offer an alternative approach. In our atomistic computer simulations, pair-wise additive interatomic potentials and O–Si–O bond bending terms are defined to model the net forces acting between atoms in the structure. Parameters for the short-range potential terms were transferred from empirical potentials originally derived to simulate periclase and quartz. The predicted structural and elastic properties of ilmenite-type $MgSiO_3$ are in good agreement with those observed. We were also able to predict the normal-mode vibrational frequencies and their associated atomic motions: the simulated Raman active bands correspond well with those observed. Bulk thermodynamic properties were calculated from the vibrational frequencies. Both the predicted heat capacity between 350 and 510 K and the entropy at 300 K of 56.13 $J \cdot mol^{-1} \cdot K^{-1}$ compare well with the measured values, but the average Grüneisen parameter of 0.9 and the volume coefficient of thermal expansion at 300 K of 1×10^{-5} K^{-1} are lower than expected, possibly because of an error in the third derivative of the Si–O potential function.

INTRODUCTION

The ilmenite-type $(Mg,Fe)SiO_3$ phase may be an important constituent of the lower transition zone and/or the top of the lower mantle of the Earth (Weidner and Ito, 1985). In phase-equilibria experiments it has been found to be stable in the region of 24 to 27 GPa and 1100 to 1400 °C (Ito and Yamada, 1982). A knowledge of the structural, thermodynamic, and lattice-dynamical properties of ilmenite-type $(Mg,Fe)SiO_3$ will, therefore, contribute greatly toward our understanding of both the nature of the mantle and mantle rheology. For example, it is not yet clear whether the phase transition of ilmenite-type to perovskite-type $(Mg,Fe)SiO_3$ has a positive or negative Clapeyron slope (Ito and Yamada, 1982; Watanabe, 1982; Williams et al., 1987). It is also unclear if phase transitions between spinel-type Mg_2SiO_4 and such high-pressure phases as ilmenite-type and perovskite-type $MgSiO_3$ cause a sufficiently large and sharp change in the elastic properties of the mantle to account for the 670-km seismic discontinuity or if a change in chemical composition is also required (see, for example, Jeanloz and Thompson, 1983).

There are considerable problems involved in the synthesis of sufficiently large quantities of ilmenite-type $(Mg,Fe)SiO_3$ to enable experimental studies to be performed, but some data are available. The structure of ilmenite-type $MgSiO_3$ has been determined by Horiuchi et al. (1982) using single-crystal X-ray diffraction. The oxygen atoms are arranged in a distorted hexagonally close-packed array while the Mg and Si cations are completely ordered and lie in the octahedral interstices (see Fig. 1). The space group, $R\bar{3}$, may be indexed in the hexagonal system with six formula units per unit cell, or in the rhombohedral system giving a primitive cell containing two formula units. The unit-cell parameters for the hexagonal cell, together with the Mg–O and Si–O bond lengths, are given in Table 1. The elastic constants have been determined by Weidner and Ito (1985) using Brillouin spectroscopy and are also presented in Table 1. The molar heat capacity between 350 and 510 K has been measured by Watanabe (1982), and the entropy at 298 K and 0.1 MPa has been calculated to be 53.18 $J \cdot mol^{-1} \cdot K^{-1}$. Ross and McMillan (1984) and McMillan and Ross (1987) have measured the ilmenite-type $MgSiO_3$ Raman sprectrum.

As an alternative approach to direct experimental study, we have developed an atomistic model of ilmenite-type $MgSiO_3$, from which its physical and thermodynamic properties can be derived. Similar atomistic computer-simulation techniques have been successfully used to predict the structural, elastic, lattice-dynamical, and thermodynamic properties of a variety of solids (see, for example, Price et al., 1987a; Catlow et al., 1985; Parker, 1983a; Post and Burnham, 1986; Matsui and Busing, 1984). In this paper we show how well the structure of

0003–004X/88/0304–0224$02.00

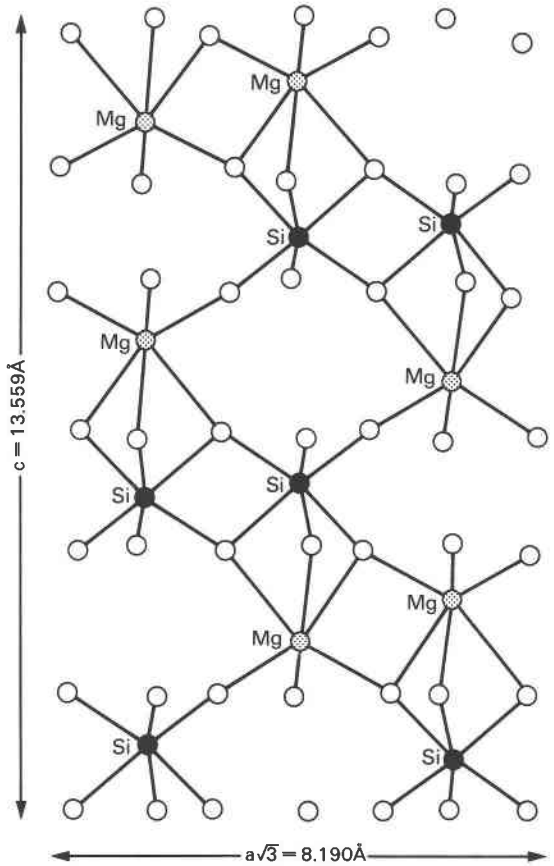

Fig. 1. A perspective view of the ilmenite-type structure of $MgSiO_3$ after Horiuchi et al. (1982). Open circles, oxygen; shaded circles, Mg; black circles, Si.

ilmenite-type $MgSiO_3$ is simulated by our model, and then we proceed to calculate its normal-mode vibrational frequencies and their associated eigenvectors. Finally, we use the normal-mode frequencies to calculate the heat capacity, entropy, average Grüneisen parameter, and coefficient of thermal expansion at temperatures between 0 and 1000 K.

Computer-simulation techniques

Ideally, the physical properties of a solid can be obtained from an explicit solution of the Schrödinger equation. For silicates this approach is not yet practicable, and our computer simulations therefore consider the structure at an atomistic level; interatomic potentials are defined to simulate the net forces acting between atoms in the structure (Stoneham, 1985). Such forces, including contributions from ionic, covalent, and van der Waals interactions, are usually assumed to be pair-wise additive. Even though this approach results in a greatly simplified model, it has been used with considerable success to investigate the structural, defect, and lattice-dynamical properties of solids.

TABLE 1. Comparison of the observed and simulated structural and elastic properties of ilmenite-type $MgSiO_3$

	Observed	THB1	THB1M
a	4.7284(4)	4.7250	4.8149
c	13.5591(16)	13.5660	13.6106
V	262.54	262.29	273.27
*I**		0.005	0.077
Si–O (3)	1.830(2)	1.820	1.856
Si–O (3)	1.768(2)	1.749	1.793
*I**		0.015	0.026
Mg–O (3)	2.163(2)	2.234	2.240
Mg–O (3)	1.990(2)	1.980	1.991
*I**		0.051	0.054
C11	472(4)	561	551
C33	382(8)	379	357
C44	106(2)	87	84
C66	152(4)	155	159
C12	168(6)	252	232
C13	70(7)	113	110
C14	27(2)	37	37
C25	24(3)	34	23
K	212	273	263

Note: Unit-cell parameters and bond lengths in Å or Å³ as appropriate; experimental data from Horiuchi et al. (1982). Elastic constants and bulk moduli (*K*) are in GPa; experimental data from Weidner and Ito (1985).
* *I* = root-mean-square error in Å.

In silicates, the major contribution to the cohesive energy is from the electrostatic or Coulombic term:

$$U_C = \tfrac{1}{2} \sum_{i}^{\text{one cells}} \sum_{j \neq i}^{\text{all cells}} q_i q_j r_{ij}^{-1},$$

where q_i and q_j are point charges on the species i and j and r_{ij} is the distance between them. This term decays slowly with distance and must be effectively summed to infinity. This is achieved by using the Ewald method (see, for example, Parker, 1983b; Catlow and Mackrodt, 1982).

It is also necessary to include a term that models both the short-range repulsive forces and the attractive dispersion forces between ions. In our studies, a Buckingham potential is used to describe these interactions:

$$U_R = \tfrac{1}{2} \sum_{i}^{\text{one cell}} \sum_{j \neq i}^{\text{all cells}} A_{ij} \exp(-r_{ij}/\rho_{ij}) - C_{ij} r_{ij}^{-6},$$

where A_{ij} and ρ_{ij} are the repulsive parameters and C_{ij} is the dispersion coefficient that must be derived for each pair of species i and j.

The effect of ionic polarizability can be simulated by using a shell model. The atom is modeled as having a core containing all the mass, surrounded by a shell of charge Y, representing the outer valence-electron cloud. The core and shell are coupled by a harmonic spring such that

$$U_S = k_{S,i} r_i^2,$$

where U_S is the core-shell interaction on ion i, $k_{S,i}$ is the spring constant, and r_i is the core-shell separation. The free-ion polarizability (α) is given by the term

$$\alpha = Y_i^2/(k_{S,i}).$$

The Si–O bond in silicates is unlikely to be fully ionic, but will include a directional covalent contribution. In ilmenite-type $MgSiO_3$ we have accounted for this, in some measure, by including a bond-bending term to simulate the directional nature of the nearly 90° O–Si–O bonds in the SiO_6 octahedra. This term has the form

$$U_B = \tfrac{1}{2} \sum_{i,j,k} k_{B,ijk}(\theta_{ijk} - \theta_O)^2,$$

where $k_{B,ijk}$ is the spring constant, θ_{ijk} is the O–Si–O bond angle, and θ_O is the octahedral angle (90°) (Leslie, 1985).

The above interatomic potential terms were used in the computer code THBREL, which minimizes the first derivative of the static cohesive energy with respect to the atomic positions to obtain the minimum-energy structure. The elastic constants and the high-frequency and static dielectric constants were then calculated by using the second derivative of the lattice energy with respect to both the atomic positions and the bulk strain. Using the above relationships to simulate a structure results in a purely static simulation, which is effectively at a temperature of 0 K. The dynamical effects of temperature can be included in simulations either explicitly using molecular dynamic codes or implicitly, as in this work, by simulating the lattice dynamics to provide a description of the vibrational frequencies and associated atomic motions. The relationships on which these lattice-dynamical calculations are based are briefly outlined below, but for a more detailed account of this theory see, for example, Price et al. (1987a), Born and Huang (1954), Ziman (1972), and Cochran (1973).

The vibrational frequencies, $\omega(\mathbf{q})$, of a lattice are related to the interatomic potential in the following way:

$$m\omega^2(\mathbf{q})\mathbf{e}(\mathbf{q}) = \mathbf{D}(\mathbf{q})\mathbf{e}(\mathbf{q})$$

where m is the ionic mass, $\mathbf{q}$ is the reciprocal-lattice wave vector for lattice waves, $\mathbf{e}(\mathbf{q})$ is the polarization vector describing the atomic displacement involved in the vibration, and $\mathbf{D}(\mathbf{q})$ is the dynamical matrix given by

$$\mathbf{D}(\mathbf{q}) = \sum_{ij} (\partial^2 U/\partial \mathbf{u}_i \partial \mathbf{u}_j) \cdot \exp(i\mathbf{q} \cdot \mathbf{R})$$

where $\mathbf{R}$ is the interatomic separation, and $\mathbf{u}_i$ and $\mathbf{u}_j$ are the atomic displacements from their equilibrium position. For a unit cell containing n atoms, there are $3n$ solutions for a given value of $\mathbf{q}$. We used the computer code THBPHON to calculate both the eigenvalues ($\omega^2(\mathbf{q})$) from which the vibrational frequencies (ω) are derived and the eigenvectors that give the atomic displacements associated with each mode ($\mathbf{e}_x(\mathbf{q})$, $\mathbf{e}_y(\mathbf{q})$, and $\mathbf{e}_z(\mathbf{q})$).

Derivation of interatomic potentials

The ability of an interatomic potential to model accurately the net interatomic forces in a solid is crucial to the success of an atomistic simulation, and considerable care must therefore be taken in deriving suitable values for the interatomic potential parameters A_{ij}, ρ_{ij}, and C_{ij}. One approach is to use ab initio potentials, such as modified electron-gas potentials (see, for example, Gordon and Kim, 1972; Wolf and Bukowinski, 1985; Post and Burnham, 1986) or Hartree-Fock methods (Catlow and Hayns, 1972; Catlow, 1977). The alternative is to derive the parameters empirically by fitting them to known properties such as the atomic structure, elastic constants, and static or high-frequency dielectric constants (see, for example, Price and Parker, 1984; Matsui et al., 1987). So far, empirical potentials have generally been able to reproduce the structural and elastic properties of a solid more accurately than ab initio potentials (Stoneham, 1985).

The terms of an interatomic potential should be able to describe the interatomic interactions in a variety of different structures, within defined limits of geometry and ranges of phenomena (Stoneham, 1985). This characteristic of "transferability" is particularly important for the simulation of solids for which there are limited experimental data, such as the high-pressure, mantle-forming silicates. In this work, we used a transfer potential, THB1 (the parameters of which are given in Table 2) to model ilmenite-type $MgSiO_3$. The Mg-O terms in THB1 were empirically derived by fitting to the experimental data of periclase (Lewis, 1985). The Si–O terms, including a shell model for oxygen and a bond-bending term for the tetrahedral O–Si–O bond, were also derived empirically by fitting to the structural and elastic constants of quartz (Sanders et al., 1984). The $O^- \cdots O^-$ interaction was derived by Catlow (1977) using Hartree-Fock methods. This potential has been successfully transferred to model the structural, elastic, and lattice-dynamical properties of forsterite (Price et al., 1987a). The forsterite structure and ilmenite-type structure are similar in that they both have oxygen ions in a distorted, hexagonally close-packed array and Mg ions in sixfold coordination. However, in forsterite the Si ions are in tetrahedral coordination whereas in ilmenite-type $MgSiO_3$ they are in octahedral coordination. In an attempt to simulate this difference, the A_{Si-O} term has been scaled from fourfold to sixfold coordination using the Huggins-Mayer relationship (Lewis, 1985; Parker, 1983b):

$$A_{oct} = A_{tet}\exp(-\Delta r/\rho),$$

where Δr is the difference in the Si ionic radius in fourfold and sixfold coordination. This gave a new A_{Si-O} term of 1383.7 eV, which was incorporated into potential THB1 to give a second potential, THB1M. The bond-bending spring constant was transferred from the tetrahedral O–Si–O bond to the octahedral O–Si–O bond without alteration.

Comparison of the observed and simulated ilmenite-type $MgSiO_3$ structure

The results of using potentials THB1 and THB1M in the computer code THBREL to simulate the structure and elastic constants of ilmenite-type $MgSiO_3$ at 0 K and zero pressure are presented in Table 1. Potential THB1 predicts the known structural and elastic properties of il-

TABLE 2. Interatomic potential parameters for THB1

A_{Mg-O} (eV) 1428.5		ρ_{Mg-O} (Å) 0.2945	
A_{Si-O} (eV) 1283.9		ρ_{Si-O} (Å) 0.3205	C_{Si-O} (eV·Å^6) 10.66
A_{O-O} (eV) 22764.3		ρ_{O-O} (Å) 0.1490	C_{O-O} (eV·Å^6) 27.88
k_S (eV·Å^{-2}) 74.92		k_B (eV·rad^{-2}) 2.09	
q_{Mg} +2.0	q_{Si} +4.0	$q_{O,core}$ +0.848	$q_{O,shell}$ −2.848

Note: Mg–O terms from Lewis (1985); Si–O terms from Sanders et al. (1984); O–O terms from Catlow (1977).

menite-type $MgSiO_3$ nearly as well as it does those of forsterite (Price et al., 1987a). Potential THB1 simulates the ilmenite-type $MgSiO_3$ unit-cell constants more accurately than THB1M; the root-mean-square (rms) errors for THB1 and THB1M are 0.005 Å and 0.077 Å, respectively. Both potentials predict the Si–O bond lengths more accurately than the Mg–O bond lengths, a feature that is inherent in the potential, as similar effects were observed in the forsterite simulations. THB1 and THB1M predict bulk moduli (K) that are about 25% stiffer than the bulk modulus of 212 GPa measured by Weidner and Ito (1985). However, the elastic constants predicted by THB1M are slightly less stiff than those predicted by THB1.

These results show that potential THB1 may be successfully transferred from periclase and quartz to model not only the structural and elastic properties of forsterite, but also those of ilmenite-type $MgSiO_3$. The difference between potentials THB1M and THB1 appears to be small. In the following section, we present a simulation of the lattice dynamics of ilmenite-type $MgSiO_3$, which provides a much more rigorous test of the interatomic potentials than structural simulations.

Vibrational-frequency calculations

There are 10 atoms in the primitive ilmenite-type unit cell, and, therefore, there are 30 normal-mode frequencies. Our calculations are carried out with $\mathbf{q}$ close to zero, and so the predicted frequencies are characteristic of those observed in the Raman and infrared spectra. Also, at the center of the Brillouin zone, ($\mathbf{q} = 0$), three of these modes are purely translational (acoustic). The irreducible representation of the other 27 optical modes is

$$\Gamma_{MgSiO_3} = 5A_g^R + 5E_g^R + 4A_u^{IR} + 4E_u^{IR}$$

(Ross and McMillan, 1984), where A modes are nondegenerate and E modes are doubly degenerate. Fifteen of these modes will be Raman active (marked R), giving ten spectral bands, and twelve will be infrared active (marked IR), giving eight absorption bands.

The normal-mode frequencies predicted using potentials THB1 and THB1M differ by less than 4%, and hence only those simulated using THB1M are shown in Table 3. The symmetry of the modes has been assigned by analysis of the eigenvectors. The Raman frequencies of ilmenite-type $MgSiO_3$ measured by McMillan and Ross (1987) are included in Table 3 and Figure 2 for comparison. There is close agreement between the measured and predicted Raman frequencies; most of the predicted frequencies are within 20 cm^{-1} and all are within 40 cm^{-1} of those measured experimentally. However, McMillan and Ross (1987) were only able to identify nine of the ten Raman bands. From our predicted Raman frequencies, the tenth band would be expected to occur around 721 cm^{-1}.

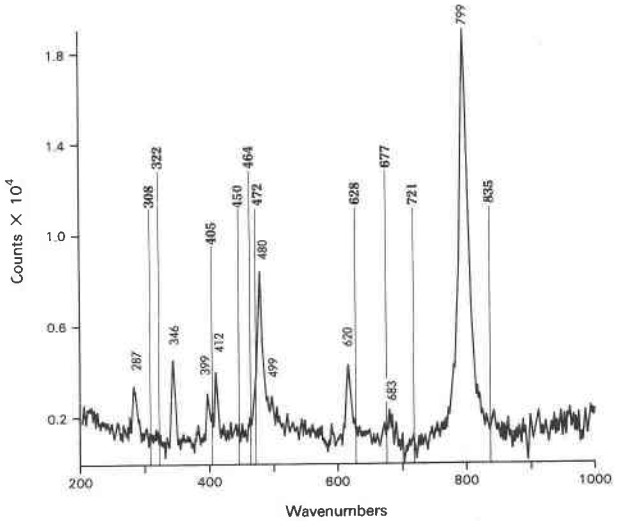

Fig. 2. The predicted Raman spectrum of ilmenite-type $MgSiO_3$ (bold numbers) superimposed on the observed Raman spectrum (McMillan and Ross, 1987).

The eigenvectors of the individual ion displacements for the Raman modes are plotted in Figure 3. Although it is doubtful whether these vibrations can be analyzed in terms of isolated groups of atoms such as the SiO_6 or MgO_6 units (Ross and McMillan, 1984), the highest frequencies (above 600 cm^{-1}) do involve motion of the Si and oxygen atoms only. Thus, it may be possible to compare the high-frequency bands of ilmenite-type $MgSiO_3$ to other structures containing SiO_6 octahedra. For example, Williams et al. (1987) have compared the observed high-frequency (above 450 cm^{-1}) bands in the infrared and Raman spectra of perovskite-type $MgSiO_3$ with the Raman spectra of synthetic stishovite and ilmenite-type $MgSiO_3$. The relevant observed vibrational frequencies of perovskite-type $MgSiO_3$ and stishovite are included in Table 3. The observed perovskite-type $MgSiO_3$ bands compare well with the ilmenite-type $MgSiO_3$ bands. For perovskite-type $MgSiO_3$ Williams et al. (1987) attributed the highest infrared active band at 797 cm^{-1} to asymmetric stretching of the SiO_6 octahedra, the lower infrared active bands at 683, 614, and 544 cm^{-1} to symmetric stretching and bending motions of the SiO_6 octahedra, and the Raman active band at 499 cm^{-1} to breathing motion of the SiO_6 octahedra. Examination of Figure

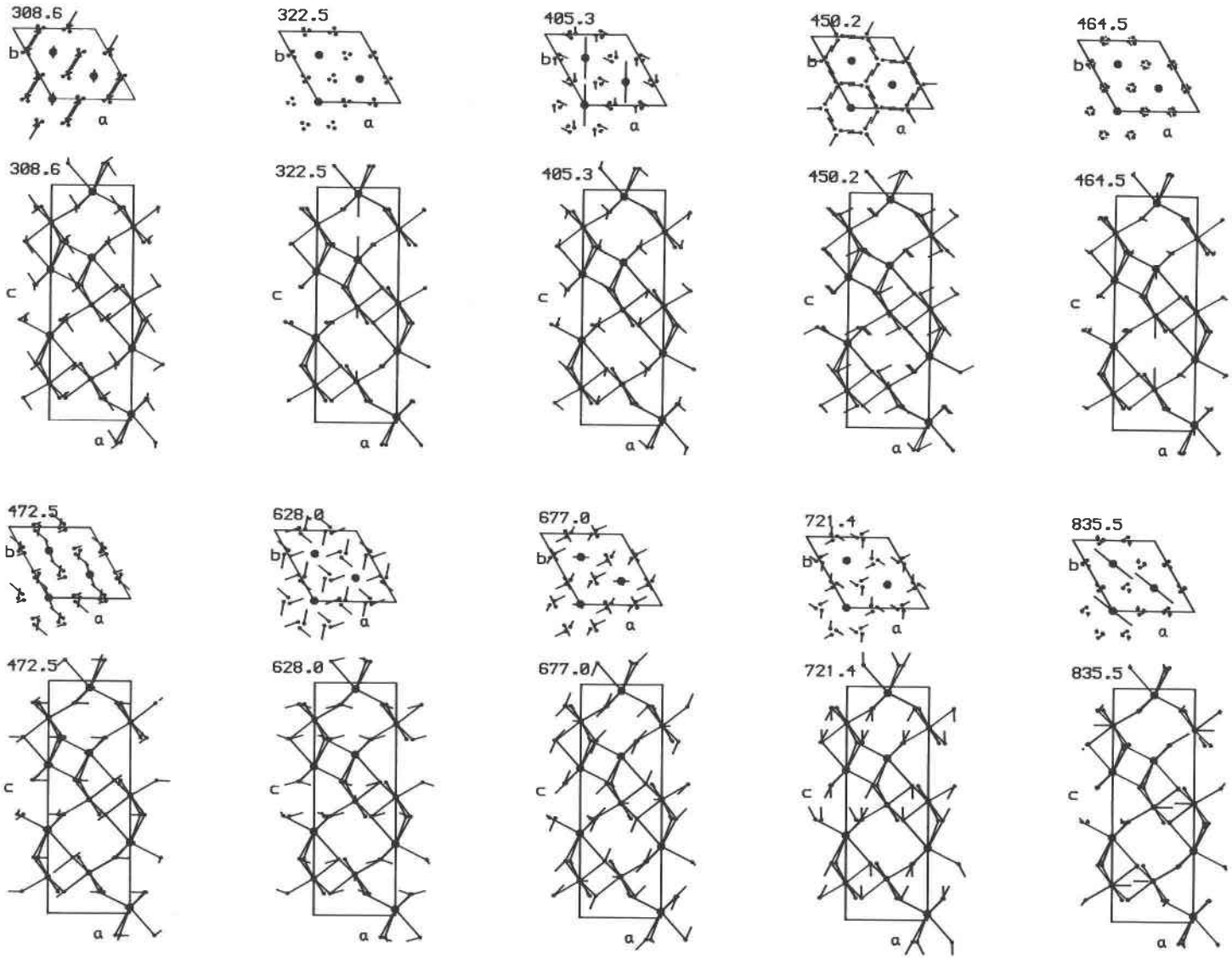

Fig. 3. The predicted Raman modes of ilmenite-type $MgSiO_3$ for $\mathbf{q}$ = (0.0, 0.0, 0.001) in the hexagonal unit cell; only one of each of the degenerate modes is shown. Largest black dots, Mg; medium-sized dots, Si; smallest dots, oxygen. The Si–O and Mg–O bonds in the SiO_6 and MgO_6 octahedra are joined in the *a*-*c* projection.

TABLE 3. Comparison of observed and predicted vibrational frequencies

Mode assignments for ilmenite-type $MgSiO_3$	Simulated ilmenite-type $MgSiO_3$ frequencies	Observed ilmenite-type $MgSiO_3$ Raman bands*	Perovskite-type $MgSiO_3$ bands**	Stishovite bands†
E_g	309	287		
A_g	323	346		
E_g	405	399		
A_g	450	412		
A_g	465	480		
E_g	473	499	499‡	
A_g	628	620	614§	
E_g	677	683	683§	
A_g	721	—		
E_g	836	799	797§	753‡
A_u	303–390			
E_u	354–403			
E_u	446–458			
A_u	481–593			
E_u	587–591		544§	589‡
E_u	665–859			
A_u	704–708			
A_u	998–1027			967‡

Note: Frequencies in wavenumbers (cm^{-1}).
* McMillan and Ross (1987).
** Williams et al. (1987).
† Hemley et al. (1986).
‡ Raman active.
§ Infrared active.

3 shows that the comparable predicted frequencies for ilmenite-type $MgSiO_3$ at 835, 677, and 628 cm^{-1} involve motion of Si and oxygen atoms, but that the Raman active mode at 472 cm^{-1} involves the motion of Mg as well as oxygen atoms. Any correlation between the stishovite and ilmenite-type $MgSiO_3$ spectra is less obvious, but the predicted ilmenite-type $MgSiO_3$ infrared bands at 587–591 cm^{-1} and 998–1027 cm^{-1} are of similar value to the stishovite Raman bands at 589 and 967 cm^{-1}.

The success of interatomic potentials THB1 and THB1M in predicting the normal-mode frequencies means that we are now able to use them to calculate some of the bulk thermodynamic properties of ilmenite-type $MgSiO_3$.

CALCULATION OF THERMODYNAMIC PROPERTIES

In order to be able to calculate bulk thermodynamic properties, information on vibrational frequencies across the whole Brillouin zone is required. The vibrational frequencies were calculated for a grid of five points in the Brillouin zone from which the density-of-states function, $G(\omega)$, was calculated. The contribution of each point in the grid to the density-of-states function was weighted by the multiplicity of the star of lattice vectors to which that point belonged. [Very similar results were obtained using grids of 8 and 27 points for ilmenite-type $MgSiO_3$; see Price et al. (1987b) for a discussion of the number of points in the Brillouin zone used to calculate the thermodynamic properties of forsterite.]

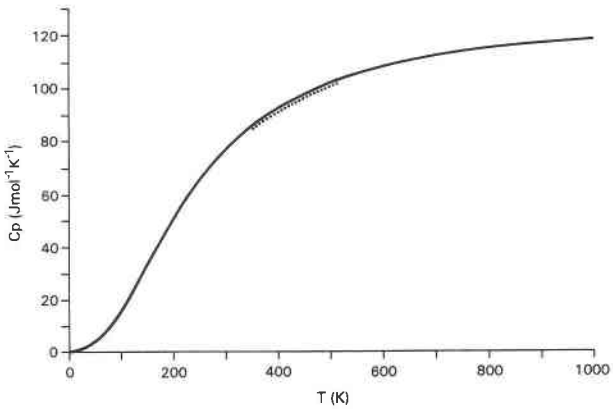

Fig. 4. A comparison of the predicted and measured heat capacity (dotted) of ilmenite-type $MgSiO_3$. The measured heat capacities are from Watanabe (1982).

The heat capacity at constant volume, C_V, is related to the normal-mode frequences by

$$C_V = dU/dT = k_B \int_0^{\omega_m} (h\omega/k_BT)^2 \cdot [\exp(h\omega/k_BT)G(\omega)\, d\omega]/[\exp(h\omega/k_BT) - 1]^2,$$

where k_B and h are Boltzmann's and Planck's constants, respectively, T is the absolute temperature, ω_m is the maximum frequency, and $G(\omega)d\omega$ is the number of modes with a frequency between ω and $\omega + d\omega$. The mode Grüneisen parameters, $\gamma_i(\mathbf{q})$, provide a measure of the response of the vibrational frequencies to compression and are given by

$$\gamma_i(\mathbf{q}) = -V/\omega_i(\mathbf{q}) \cdot [d\omega_i(\mathbf{q})/dV].$$

TABLE 4. Predicted thermodynamic properties of ilmenite-type $MgSiO_3$

T (K)	C_V ($J \cdot mol^{-1} \cdot K^{-1}$)	$\bar{\gamma}$	β ($\times 10^{-5}$ K^{-1})	C_P ($J \cdot mol^{-1} \cdot K^{-1}$)	S ($J \cdot mol^{-1} \cdot K^{-1}$)
100	15.96	1.1878	0.2628	15.96	7.66
200	51.68	1.0311	0.7387	51.76	29.80
300	77.57	0.9696	1.0426	77.80	56.13
400	93.00	0.9393	1.2109	93.42	80.84
500	102.23	0.9228	1.3078	102.85	102.79
600	108.01	0.9106	1.3634	108.81	122.11
700	111.80	0.9045	1.4017	112.78	139.20
800	114.39	0.9046	1.4346	115.58	154.45
900	116.24	0.9017	1.4530	117.61	168.19
1000	117.60	0.8995	1.4665	119.15	180.66

The average Grüneisen parameter, $\bar{\gamma}$ (Kieffer, 1982), is given by

$$\bar{\gamma} = 1/C_V \sum_i (C_V)_i \cdot \omega_i,$$

where $(C_V)_i$ is the contribution to the heat capacity made by each mode, i. The following relationships were used to calculate the thermal-expansion coefficient (β), the heat capacity at constant pressure (C_P), and the entropy (S_P):

$$\beta = \bar{\gamma} C_V / KV$$
$$C_P = C_V + KT\beta^2 V$$
$$S_P = \int_0^T C_P/T \cdot dT,$$

where V is the molar volume and K is the bulk modulus. The vibrational-mode frequencies were calculated at pressures of 0 and 5 GPa to evaluate $d\omega_i$.

The simulated thermodynamic properties for temperatures between 0 and 1000 K are shown in Table 4. The predicted heat capacity, C_P, is compared with the heat capacity measured by Watanabe (1982) in Figure 4. Over the range of experimental results available, 350 to 510 K, the agreement between the measured and predicted heat capacities is very good—within 2% if the measured value of 212 GPa (Weidner and Ito, 1985) is used for K (or within 1.5% using the predicted value of 263 GPa). Also, the predicted entropy at 300 K of 56.13 $J \cdot mol^{-1} \cdot K^{-1}$ is within the quoted error of the entropy at 298 K of 53.18 ± 3.26 $J \cdot mol^{-1} \cdot K^{-1}$ calculated by Watanabe (1982). However, the predicted average Grüneisen parameters are probably too low. No measured Grüneisen parameters are available for ilmenite-type $MgSiO_3$, but Williams et al. (1987) have pointed out that if the ilmenite-type to perovskite-type phase transition of $MgSiO_3$ in the mantle has a negative Clapeyron slope (as predicted by the phase-equilibria data of Ito and Yamada (1982)), the average Grüneisen parameter of ilmenite-type $MgSiO_3$ would be expected to be within 85% of the average Grüneisen parameter of perovskite-type $MgSiO_3$. Williams et al. (1987) calculated the Grüneisen parameter of perovskite-type $MgSiO_3$ from just the mid-infrared spectra to be 1.36 ± 0.15—considerably higher than the Grüneisen parameter of 0.9 predicted for ilmenite-type $MgSiO_3$. Potential THB1 produced a similar underestimation of the average Grüneisen parameter when used to simulate forsterite (Price et al., 1987b), the average high-temperature Grüneisen parameter of forsterite being predicted to be 0.88 rather than the measured value of 1.1. Price et al. (1987b) attributed this to a systematic error in the third derivative of the Si-O potential function. However, this discrepancy does not cause serious errors in the predicted heat capacity and entropy calculated using the average Grüneisen parameter, but does cause an underestimate of the high-temperature thermal-expansion coefficient.

Conclusions

The empirical interatomic potential THB1 can be successfully transferred from quartz and periclase, to which it was originally fitted, to simulate the structural and elastic properties of both forsterite and ilmenite-type $MgSiO_3$. Scaling the A_{Si-O} term according to the difference in Si ionic radius in tetrahedral and octahedral coordination had only a small effect on the predicted properties of ilmenite-type $MgSiO_3$. The vibrational frequencies are also predicted accurately, although only the Raman spectrum (McMillan and Ross, 1987) is available for comparison. However, the ability of such potentials to predict the vibrational frequencies across the whole Brillouin zone can be measured by calculating the bulk thermodynamic properties. The predicted values of the heat capacity between 350 and 510 K (see Fig. 4) and the entropy at 300 K of 56.13 $J \cdot mol^{-1} \cdot K^{-1}$, agree well with those measured by Watanabe (1982), but the average Grüneisen parameter and the volume thermal-expansion coefficient are lower than expected, possibly because of an error in the third derivative of the Si-O potential function (Price et al., 1987b).

Atomistic potentials establish a link between microscopic and macroscopic phenomena, enabling the prediction of bulk properties and the investigation of phase relations. However, although potential THB1 has proved to be transferable to forsterite and ilmenite-type $MgSiO_3$, the wider use of this method of deriving interatomic potential parameters may be limited. In particular, empirical potentials may become unstable at interatomic separations that differ significantly to those for which they were fitted, conditions likely to occur in the study of high pressure–high temperature structures or point defects. Therefore, in the future it may prove necessary to improve further the ab initio methods of interatomic potential derivation, such as those used by Hemley et al. (1987) and Wolf and Bukowinski (1987), in order to be able to accurately predict the properties of the high-density mantle phases for which there is little experimental data. In the meantime, however, empirical potentials still provide the best way of simulating the geophysically important properties of mantle-forming silicates.

Acknowledgments

We would like to thank the SERC for the programs THBREL and THBPHON, which are supported at their Daresbury laboratory; N. L. Ross for a copy of the ilmenite-type $MgSiO_3$ Raman spectra; J. R. Baker for drafting the figures; and J. E. Post, M.S.T. Bukowinski, and N. L. Ross for their helpful reviews of the manuscript. A.W. gratefully acknowledges receipt of a NERC studentship and G.D.P. receipt of a Royal Society Research Fellowship and NERC research grants GR3/5993 and GR3/6358.

References cited

Born, M., and Huang, K. (1954) Dynamical theory of crystal lattices. Clarendon Press, Oxford.

Catlow, C.R.A. (1977) Point defect and electronic properties of uranium dioxide. Royal Society of London Proceedings, A353, 533–561.

Catlow, C.R.A., and Hayns, M.R. (1972) A computational study of the

F^--F^- interionic potential. Journal of Physics C, Solid State Physics, 5, L237–L240.

Catlow, C.R.A., and Mackrodt, W.C. (1982) Computer simulation of solids. Lecture notes in physics, 166. Springer-Verlag, Berlin.

Catlow, C.R.A., Freeman, C.M., and Royle, R.L. (1985) Recent studies using static simulation techniques. Physica, 131B, 1–12.

Cochran, W. (1973) The dynamics of atoms in crystals. Edward Arnold, London.

Gordon, R.G., and Kim, Y.S. (1972) A theory for the forces between closed-shell atoms and molecules. Journal of Chemical Physics, 56, 3122–3133.

Hemley, R.J., Mao, H-K., Bell, P.M., and Akimoto, S. (1986) Lattice vibrations of high-pressure phases: Raman spectrum of synthetic stishovite. Physica, 139 & 140B, 455–457.

Hemley, R.J., Jackson, M.D., and Gordon, R.G. (1987) Theoretical study of the structure, lattice dynamics, and equations of state of the perovskite-type $MgSiO_3$ and $CaSiO_3$. Physics and Chemistry of Minerals, 14, 2–12.

Horiuchi, H., Hirano, M., Ito, E., and Matsui, Y. (1982) $MgSiO_3$ (ilmenite-type): Single crystal X-ray diffraction study. American Mineralogist, 67, 788–793.

Ito, E., and Yamada, H. (1982) Stability relations of silicate spinels, ilmenites, and perovskites. In S. Akimoto and M.H. Manghnani, Eds., High-pressure research in geophysics, p. 405–419. Centre for Academic Publications, Tokyo, Japan.

Jeanloz, R., and Thompson, A.B. (1983) Phase transitions and mantle discontinuities. Reviews in Geophysics and Space Physics, 21, 51–74.

Kieffer, S.W. (1982) Thermodynamics and lattice vibrations of minerals: 5. Applications to phase equilibria, isotope fractionation and high-pressure thermodynamic properties. Reviews of Geophysics and Space Physics, 20, 827–849.

Leslie, M. (1985) A three-body potential model for the static simulation of defects in ionic crystals. Physica, 131B, 145–150.

Lewis, G.V. (1985) Interatomic potentials: Derivation of parameters for binary oxides and their use in ternary oxides. Physica, 131B, 114–118.

Matsui, M., and Busing, W.R. (1984) Computational modeling of the structure and elastic constants of the olivine and spinel forms of Mg_2SiO_4. Physics and Chemistry of Minerals, 11, 55–59.

Matsui, M., Akaogi, M., and Matsumoto, T. (1987) Computational model of the structural and elastic properties of the ilmenite and perovskite phases of $MgSiO_3$. Physics and Chemistry of Minerals, 14, 101–106.

McMillan, P., and Ross, N.L. (1987) Heat capacity for Al_2O_3 corundum and $MgSiO_3$ ilmenite. Physics and Chemistry of Minerals, 14, 225–234.

Parker, S.C. (1983a) Prediction of mineral crystal structures. Solid State Ionics, 8, 179–186.

——— (1983b) Computer modelling of minerals. Ph.D. thesis, University of London, London, U.K.

Post, J.E., and Burnham, C.W. (1986) Ionic modeling of mineral structures and energies in the electron gas approximation: TiO_2 polymorphs, quartz, forsterite, diopside. American Mineralogist, 71, 142–150.

Price, G.D., and Parker, S.C. (1984) Computer simulations of the structural and physical properties of the olivine and spinel polymorphs of Mg_2SiO_4. Physics and Chemistry of Minerals, 10, 209–216.

Price, G.D., Parker, S.C., and Leslie, M. (1987a) The lattice dynamics of forsterite. Mineralogical Magazine, 51, 157–170.

——— (1987b) Computer prediction of the thermodynamic properties of Mg_2SiO_4 polymorphs. Physics and Chemistry of Minerals, 15, 181–190.

Ross, N.L., and McMillan, P. (1984) The Raman spectrum of $MgSiO_3$ ilmenite. American Mineralogist, 69, 719–721.

Sanders, M.J., Leslie, M., and Catlow, C.R.A. (1984) Interatomic potentials for SiO_2. Journal of the Chemical Society, Chemical Communications, 1271–1273.

Stoneham, A.M. (1985) Interatomic potentials for condensed matter. Physica, 131B, 69–73.

Watanabe, H. (1982) Thermochemical properties of synthetic high-pressure compounds relevant to the Earth's mantle. In S. Akimoto and M.H. Manghnani, Eds., High-pressure research in geophysics, p. 441–464. Centre for Academic Publications, Tokyo, Japan.

Weidner, D.J., and Ito, E. (1985) Elasticity of $MgSiO_3$ in the ilmenite phase. Physics of the Earth and Planetary Interiors, 40, 65–70.

Williams, Q., Jeanloz, R., and McMillan, P. (1987) Vibrational spectrum of $MgSiO_3$-perovskite: Zero pressure Raman and mid-infrared spectra to 27 GPa. Journal of Geophysical Research, 92, 8116–8128.

Wolf, G.H., and Bukowinski, M.S.T. (1985) Ab initio structural and thermoelastic properties of orthorhombic $MgSiO_3$ perovksite. Geophysical Research Letters, 12, 809–812.

——— (1987) Theoretical study of the structural properties and equations of state of $MgSiO_3$ and $CaSiO_3$ perovskites: Implications for lower mantle composition. In M. Manghnani and Y. Syono, Eds., High-pressure research in mineral physics, p. 313–335. Terra Scientific Publishing Company, Tokyo.

Ziman, J.M. (1972) Principles of the theory of solids (2nd edition). Cambridge University Press, Cambridge.

Manuscript received February 23, 1987
Manuscript accepted September 14, 1987